

## Specific heat and isothermal magnetocaloric effect in UNi<sub>0.5</sub>Sb<sub>2</sub>

T. Plackowski, D. Kaczorowski, and Z. Bukowski

*Institute of Low Temperature and Structure Research, Polish Academy of Sciences, P.O. Box 1410, 50-950 Wrocław, Poland*

(Received 10 June 2005; revised manuscript received 31 August 2005; published 15 November 2005)

Single crystals of UNi<sub>0.5</sub>Sb<sub>2</sub> have been studied by means of specific heat ( $C_p$ ) and isothermal magnetocaloric coefficient ( $M_T$ ) measurements using a heat-flow technique. The  $C_p(T)$  variation exhibits a pronounced  $\lambda$ -shaped anomaly at  $T_N=161.1$  K, associated with an antiferromagnetic phase transition. Another feature, less distinct and strongly hysteretic, was found at  $T_{tr}=63.5$  K (cooling) and 71 K (heating), which signals a change in the magnetic structure. In an applied magnetic field  $T_N$  decreases, while  $T_{tr}$  remains constant. The analysis of the zero-field anomaly at  $T_N$  indicated the effective total angular momentum  $J=1/2$  for U ions and placed UNi<sub>0.5</sub>Sb<sub>2</sub> between the two- and three-dimensional Ising systems. The  $M_T(B)$  curves measured below the onset of antiferromagnetic (AF) order revealed a  $\sim \ln|B-B_N|$  anomaly at the transition field  $B_N$ , which increases with lowering temperature. All the calorimetric data form unanimously an AF phase-transition line of the square-root type. Its shape was described by a mean-field model for the tetragonal lattice with ferromagnetic coupling ( $J$ ) in the  $ab$  plane and AF coupling along  $c$  axis ( $J_1$ ). This analysis revealed strong anisotropy in the magnetic exchange interactions with the ratio  $|J_1|/J=0.25$ .

DOI: 10.1103/PhysRevB.72.184418

PACS number(s): 75.50.Ee, 75.40.Cx, 75.30.Sg, 75.30.Kz

### I. INTRODUCTION

The ternary uranium antimonides UTSb<sub>2</sub> ( $T=3d$ -,  $4d$ -,  $5d$ -electron transition metal) crystallize in a simple tetragonal structure of the HfCuSi<sub>2</sub> type (space group  $P4/nmm$ ).<sup>1</sup> Their electronic properties have been studied in the past on polycrystalline and powder samples by means of electrical, magnetic, Mössbauer, and neutron diffraction measurements.<sup>2,3</sup> Most of the compounds were found to order magnetically at low temperatures and to reveal features in their transport behavior, which are characteristic of Kondo lattices with strongly screened magnetic moments.

Recently, we succeeded in growing large single crystals of selected UTSb<sub>2</sub> ternaries and launched a systematic reinvestigation of their physical properties. Interestingly, for a few compounds the behavior of single-crystalline specimens differs considerably from the data reported in Ref. 2. The probable reason for that is deviation from the ideal 1:1:2 stoichiometry. For example, in the case of antiferromagnetic UNiSb<sub>2</sub> ( $T_N=175$  K) the crystal structure refinement from the single-crystal x-ray data indicated a large deficiency on the crystallographic sites occupied by Ni atoms, yielding the composition UNi<sub>0.5</sub>Sb<sub>2</sub>.<sup>4</sup> Concurrently, magnetic measurements revealed more complex behavior of single crystals in comparison to polycrystalline samples, with the most notable feature, absent in the latter ones, of an order-order phase transition occurring at  $T_{tr}\approx 63$  K—i.e., much below the Néel temperature  $T_N=161$  K.<sup>3</sup> The <sup>121</sup>Sb Mössbauer studies determined the magnetic structure to be of antiferromagnetic (AF) II type, with the uranium magnetic moments pointing along the tetragonal  $c$  axis and forming (+ - - +) sequence of ferromagnetically coupled (001) planes.<sup>2</sup>

In this paper we report the results of heat-capacity measurements on a single crystal of UNi<sub>0.5</sub>Sb<sub>2</sub>, performed in an applied magnetic field, with the main emphasis on the temperature regions in the vicinity of  $T_{tr}$  and  $T_N$ . Furthermore, we discuss the isothermal magnetocaloric effect in this com-

pound in the vicinity of the AF transition. The field dependence of  $T_N$  was analyzed in terms of a simple mean-field approximation (MFA).

### II. EXPERIMENT

#### A. Sample preparation and characterization

Polycrystalline samples of UNiSb<sub>2</sub> were prepared by arc melting the elemental constituents (purity 99.99%) in a titanium-gettered argon atmosphere. In order to compensate weight losses due to evaporation some excess amounts of antimony were added beforehand.

Single crystals of UNi<sub>0.5</sub>Sb<sub>2</sub> were grown from Sb flux applying the technique developed for USb<sub>2</sub>.<sup>5</sup> Approximately 4 g of UNiSb<sub>2</sub> and 11 g of Sb were placed in a thick-wall molybdenum crucible and sealed under Ar atmosphere. The crucible was heated in vacuum in a graphite furnace up to 1200 °C, held at this temperature for 5 h and subsequently slowly (3 °C/h) cooled down to 700 °C, followed by uncontrolled inert furnace cooling down to room temperature. After opening the crucible, the excess of antimony was removed by sublimation in vacuum. Large single crystals (typically  $5\times 5\times 1$  mm<sup>3</sup>), grown on the walls, could easily be isolated.

The quality of single crystals obtained was checked by x-ray diffraction and energy-dispersive x-ray (EDX) analysis. The refined lattice parameters and the chemical composition were in agreement with those reported in Ref. 4.

Magnetic susceptibility measurements were carried out in the temperature range 1.7–300 K in an applied magnetic field of 5 T using a Quantum Design superconducting quantum interference device (SQUID) magnetometer. For these measurements a single crystal of UNi<sub>0.5</sub>Sb<sub>2</sub> was used and oriented with the magnetic field being parallel to the easy magnetization axis (i.e.,  $c$  axis).

#### B. Calorimetric measurements

Both the specific heat  $C_p$  and the isothermal magnetocaloric coefficient  $M_T$  were measured using a heat-flow

calorimeter.<sup>6</sup> In this method the sample is connected with a heat sink by means of a sensitive heat-flow meter of high thermal conductance  $K$ . In an ideal case, for  $K \rightarrow \infty$ , the sample conditions may be regarded as isothermal. Therefore, this method is located on the opposite side of the  $K$  scale than the classical adiabatic method, for which  $K \rightarrow 0$  is expected. The family of the relaxation methods is located somewhere in the middle of this scale. In the adiabatic method the heat is delivered to the sample and the temperature change is measured. In the isothermal method this is the outer temperature or the applied magnetic field which is the control parameter, whereas the energy exchanged between the sample and its surrounding is the measured output.

To sense the heat flux we used a commercial, miniature, one-stage Peltier cell with sensitivity of  $A=0.45$  V/W at room temperature (RT) and  $A=0.08$  V/W at liquid nitrogen temperature (LN<sub>2</sub>T). The sensitivity increases slightly with magnetic field (by 11% at RT for a field of 13 T applied perpendicularly to the Peltier cell surface). The thermal conductance of the cell amounts to  $K=0.028$  W/K at RT and 0.035 W/K at LN<sub>2</sub>T. The sample was fixed on the cell top plate, made of 0.5-mm-thick alumina. The bottom of the heat-flow meter was permanently attached to the heat sink (a massive copper block) of controlled temperature. An in-field calibrated Pt thermometer was attached to the sink. Such a device was surrounded by a double passive radiation screen (gold plated). Both screens were in a good thermal contact with the sink. The whole ensemble was evacuated down to  $10^{-6}$  hPa and placed in the gas-flow variable-temperature insert of an Oxford cryostat with a 13/15-T superconducting magnet.

If the temperature of the sink  $T$  varies with a constant rate  $\dot{T}$ , then (neglecting some small corrections)  $C_p$  is directly proportional to the voltage  $U$  on terminals of the heat-flow meter:

$$C_p \equiv \frac{dq}{dT} = \frac{\dot{q}}{\dot{T}} = \frac{U}{A\dot{T}}, \quad (1)$$

where  $q$  is the heat flux flowing from the sink to the sample. The heat capacity of the top plate of the Peltier cell, which has to be subtracted from the raw results, has been determined in separate experiments with calibrating Cu samples. The  $C_p$  measurements could be performed both upon cooling and heating, at any value of constant magnetic field  $B$ .

On the other hand, it is possible to stabilize the sink temperature and sweep the magnetic field at some constant rate  $\dot{B}$ . This way the magnetocaloric effect may be studied in quasi-isothermal conditions:

$$M_T \equiv \frac{dq}{dB} = \frac{-\dot{q}}{\dot{B}} = \frac{-U}{A\dot{B}}, \quad (2)$$

where  $M_T$  is the isothermal magnetocaloric coefficient. The minus was introduced to keep the convention of the heat flux direction used in the formula for  $C_p$ . The  $M_T$  measurements could be performed also upon both increasing and decreasing field. The additional advantage is a lack of any addenda contribution from the empty Peltier cell.

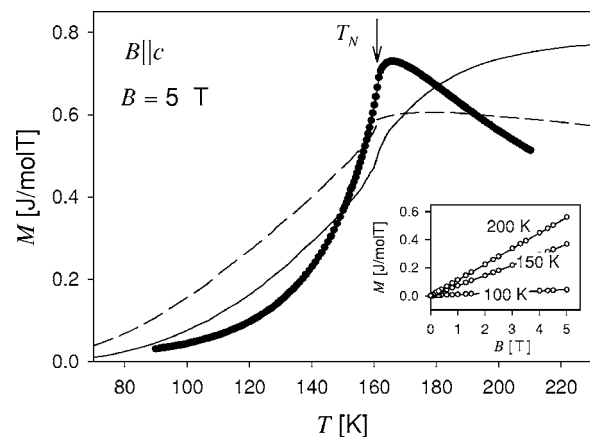


FIG. 1. Magnetization ( $M$ ) of a UNi<sub>0.5</sub>Sb<sub>2</sub> single crystal measured in the vicinity of the antiferromagnetic phase transition (dots) with magnetic field of  $B=5$  T applied along the easy axis. Thin lines show the theoretical predictions of the antiferromagnetic Ising models for two-dimensional plane square (solid line) and three-dimensional simple cubic (dashed line) lattices. (Ref. 9 and 10). These lines are scaled for the observed Néel temperature  $T_N \approx 161$  K (indicated by an arrow); along the vertical axis they are presented in arbitrary units. The inset shows the field variations of the magnetization measured at three different temperatures.

A single crystal of UNi<sub>0.5</sub>Sb<sub>2</sub> (260 mg) was glued (using GE varnish) to the Peltier cell in such a way that the easy axis (i.e., the  $c$  axis) was oriented parallel to the magnetic field. Several temperature runs 300 K  $\rightarrow$  20 K  $\rightarrow$  300 K with  $T \approx 1$  K/min rate were performed at various magnetic fields in the following order: at  $B=0, 2.5, 5, 7.5, 10, 13$ , and 0 T. The latter run was executed with  $T \approx 0.5$  K/min. Next, a series of magnetic sweeps 0 T  $\rightarrow$  13 T  $\rightarrow$  0 T were performed with a  $B=0.2$  T/min rate. Finally, another two control temperature runs were performed at  $B=0$  and 13 T with a standard  $T \approx 1$  K/min rate. During subsequent temperature runs we noticed a gradual decrease of the thermal conductance between sample and the top plate of the Peltier cell,  $K_{st}$ . Eventually, after several runs,  $K_{st}$  saturated. Thus, in order to account for the energy exchange by radiation, we applied appropriate corrections<sup>6</sup> for the specific-heat experiments. Other examples of heat-flow calorimetric measurements were given recently for UAs antiferromagnet<sup>7</sup> and YBa<sub>2</sub>Cu<sub>3</sub>O<sub>7-d</sub> high- $T_c$  superconductor.<sup>8</sup>

### III. RESULTS AND DISCUSSION

#### A. Magnetization

The temperature dependence of the dc magnetization of UNi<sub>0.5</sub>Sb<sub>2</sub> at  $B=5$  T is shown in Fig. 1, and the inset presents the  $M(B)$  dependences taken at different temperatures. The behavior is typical for antiferromagnets, with a characteristic  $\tau \ln(\tau)$ -type singularity<sup>9,10</sup> [ $\tau$  is the reduced temperature  $(T - T_N)/T_N$ ] noticed at  $T_N(B=5$  T)  $\approx 161$  K. As shown in the inset, in the vicinity of the antiferromagnetic phase transition  $M$  depends linearly on the field. Thus, the shape of the  $M(T)$  curve is field independent. In general, this shape is reminiscent of those calculated for some simple cases of the AF

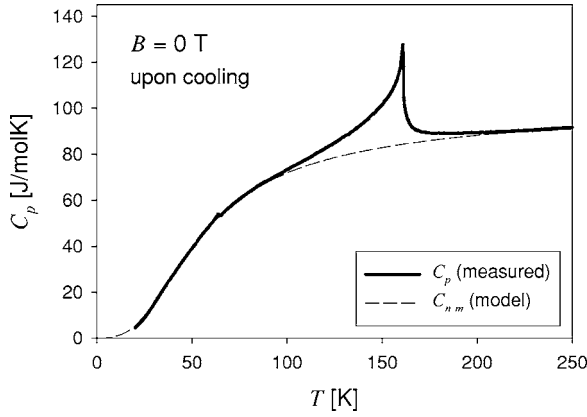


FIG. 2. Temperature dependence of the specific heat for single-crystal  $\text{UNi}_{0.5}\text{Sb}_2$ , measured with a heat-flow calorimeter upon cooling (first run). The dashed line represents a simple model ( $C_{n-m}$ ), which was used to describe all nonmagnetic contributions to the total specific heat (see the text for details).

lattices (see thin lines in Fig. 1). The similarity is closer for the three-dimensional (3D) simple cubic model, though on both sides of the transition the experimentally observed slopes are remarkably steeper.

### B. Specific heat

The temperature dependence of the specific heat of  $\text{UNi}_{0.5}\text{Sb}_2$  is presented in Fig. 2. It has a classical sigmoid shape with two anomalies superimposed. The major,  $\lambda$ -type singularity at  $T_N=161.1$  K manifests a transition to the antiferromagnetic state, in an agreement with the magnetic and electrical transport data reported in Ref. 4. In turn, the small feature at  $T_{tr}=63.5$  K corresponds to the anomalies in the temperature-dependent magnetic susceptibility and electrical resistivity, which have tentatively been attributed in Ref. 3 to a change in the magnetic structure.

In order to analyze the magnetic component in the total specific heat measured, it was assumed in the following that the nonmagnetic contributions can be described by the formula

$$C_{n-m} = 3.5C_D(T, \Theta_D) + \gamma T, \quad (3)$$

where the first term stands for the phonon contribution from 3.5-D modes per formula unit ( $\Theta_D$  is the Debye temperature), whereas the second term contains both the electronic and dilatation contributions. The  $\Theta_D$  and  $\gamma$  variables were used as fitting parameters in a Levenberg-Marquart optimization process combined with a random search. The temperature regions surrounding both the  $C_p(T)$  anomalies (57–65 K and 90–230 K, respectively) were excluded from the fitting. The best result was found for  $\Theta_D=224 \pm 3$  K and  $\gamma = 31 \pm 2$  mJ/(mol K<sup>2</sup>). We stress that this model should be treated merely as a rough approximation for nonmagnetic contributions. More reliable results could be achieved, e.g., by measuring  $C_p(T)$  for a nonmagnetic reference compound. However, within a narrow window around  $T_N$  the uncertainty could be treated as a constant and will not disturb our further analysis.

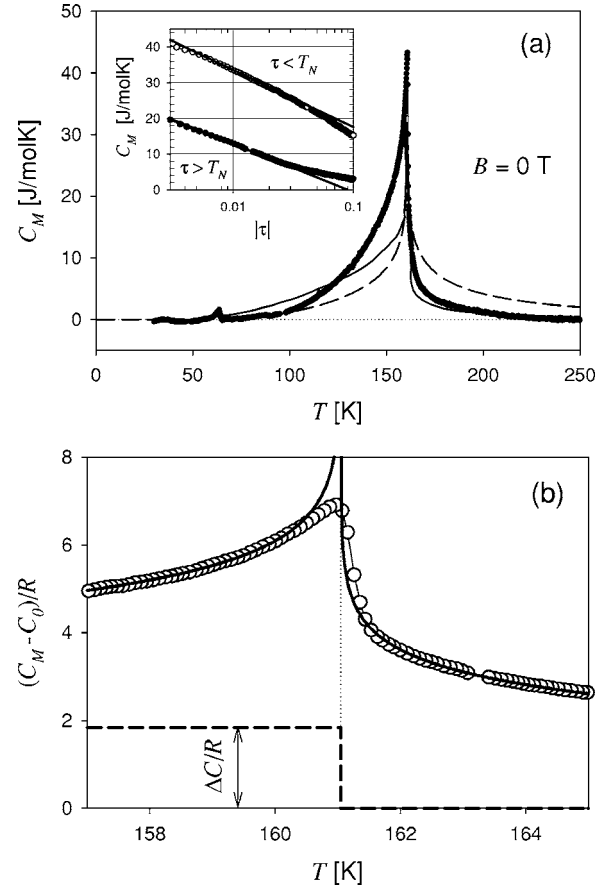


FIG. 3. (a) The magnetic contribution to the specific heat of  $\text{UNi}_{0.5}\text{Sb}_2$  at zero magnetic field. Thin lines show the theoretical predictions for the 2D (dashed line) and 3D fcc (solid line) Ising models. The inset shows the semilogarithmic plot of  $C_M$  around  $T_N=161.1$  K and fitting by the logarithmic approximation [ $\tau \equiv (T - T_N)/T_N$  is the reduced temperature]. (b)  $C_M$  (points) separated into two components: the finite jump of the height  $\Delta C/R=1.8$  (dashed line) and the weak logarithmic divergence (solid line) with the amplitude ratio  $A^+/A^-=0.84$ .  $C_0$  is an arbitrary constant.

By subtracting  $C_{n-m}$  from  $C_p$  the magnetic contribution to the specific heat ( $C_M$ ) of  $\text{UNi}_{0.5}\text{Sb}_2$  was derived [see Fig. 3(a)]. The total magnetic entropy related to the AF transition was estimated to be  $S_{\text{magn}} \approx 5.2$  J/(mol K), which is close to the value of  $R \ln 2 = 5.76$  J/(mol K) ( $R$  is the gas constant) expected for a doubly degenerated magnetic ground state. The  $\lambda$  shape of the anomaly suggests that the transition is governed by the fluctuations of the order parameter. A comparison with the  $C_p$  results for 2D and fcc 3D Ising<sup>11</sup> models reveals a general similarity (especially with the 3D case); however, it is obvious that these simple models are not sufficient to explain the behavior of strongly anisotropic  $\text{UNi}_{0.5}\text{Sb}_2$ . Nevertheless, some basic facts could be stated. In some critical region around  $T_N$  a simple power-law dependence of the specific heat is expected:

$$C_M^\pm \sim \frac{A^\pm}{\alpha} |\tau|^{-\alpha}, \quad (4)$$

where  $\tau$  is the reduced temperature,  $\alpha$  is the critical exponent,  $A^\pm$  are fluctuation amplitudes, and “+” and “−” super-

TABLE I. Parameters of the  $C_M(T)$  data fit according to Eq. (5). The value of the critical parameter  $\alpha$  is not a result of numerical procedure but it is a consequence of the choice of a particular model suitable to describe the  $C_M$  singularity.  $A^\pm$  are fluctuation amplitudes, and  $\Delta C$  is the height of the underlying specific heat jump.

$\alpha$	$0^+$
$A^+/R$	$0.71 \pm 0.03$
$A^-/R$	$0.84 \pm 0.03$
$A^+/A^-$	$0.84 \pm 0.05$
$\Delta C/R$	$1.8 \pm 0.2$

scripts refer to the high- and low-temperature sides of the transition. In the case of  $\alpha \rightarrow 0^+$  this description could be replaced by an equivalent, but more practical formula

$$C_M^- \sim C_0 + \Delta C - A^- \ln|\tau|, \quad C_M^+ \sim C_0 - A^+ \ln \tau, \quad (5)$$

where  $C_0$  is an arbitrary constant (which also contains the error made in the determination of  $C_{n-m}$ ). This approach separates the critical anomaly into a weak, logarithmic divergence and a finite jump of the height  $\Delta C$ . This jump could be analyzed in terms of the mean-field approach (for which  $\alpha = 0^-$ ). The semilogarithmic plot shown as an inset in Fig. 3(a) shows that within a  $\pm 4$  K window around  $T_N$  the magnetic specific heat diverges logarithmically, thus confirming our  $\alpha = 0^+$  presumption. This makes  $\text{UNi}_{0.5}\text{Sb}_2$  closer to the 2D Ising system ( $\alpha = 0^+$ ) than to the 3D Ising case [for which  $\alpha = 0.119$  (Ref. 12)]. The fitting parameters are presented in Table I.

We indicate that two conclusions could be derived from the above analysis. First, the height of the underlying specific-heat jump could be compared with the well-known mean-field formula

$$\Delta C/R = \frac{5J(J+1)}{J^2 + (J+1)^2}, \quad (6)$$

where  $J$  is the total angular momentum. Values of  $J=1/2$  and 1 give  $\Delta C/R=3/2$  and 2, respectively. The measured value of  $\Delta C/R=1.8$  lies in between, but with the indication given by the magnetic entropy ( $S_{\text{magn}} \approx R \ln 2$ ) we would rather point to  $J=1/2$  as the effective value for  $\text{UNi}_{0.5}\text{Sb}_2$ .

The second conclusion could be drawn from the amplitude ratio, which usually gives information on the universality class of the system. For  $\text{UNi}_{0.5}\text{Sb}_2$  this is not straightforward, since the obtained value of  $A^+/A^- = 0.84$  stays between the ratio  $A^+/A^- = 1$  for the 2D Ising model and the ratio  $A^+/A^- = 0.52-0.54$  predicted for the 3D model.<sup>13</sup> We could only notice that  $A^+/A^-$  seems to be slightly closer to the 3D case. Apparently, this ambiguity has an origin in the strong anisotropy of the investigated system. The latter problem will be addressed in Sec. III D.

The entropy jump associated with the low-temperature phase transition is as small as  $\Delta S = 0.13$  J/(mol K). Interestingly, the latter anomaly has been found highly hysteretic. As shown in Fig. 4(a), the transition temperature is equal to  $T_{tr} = 63.5$  K for measurements taken upon cooling and to  $T_{tr} = 71$  K upon heating. The hysteresis suggests a first-order

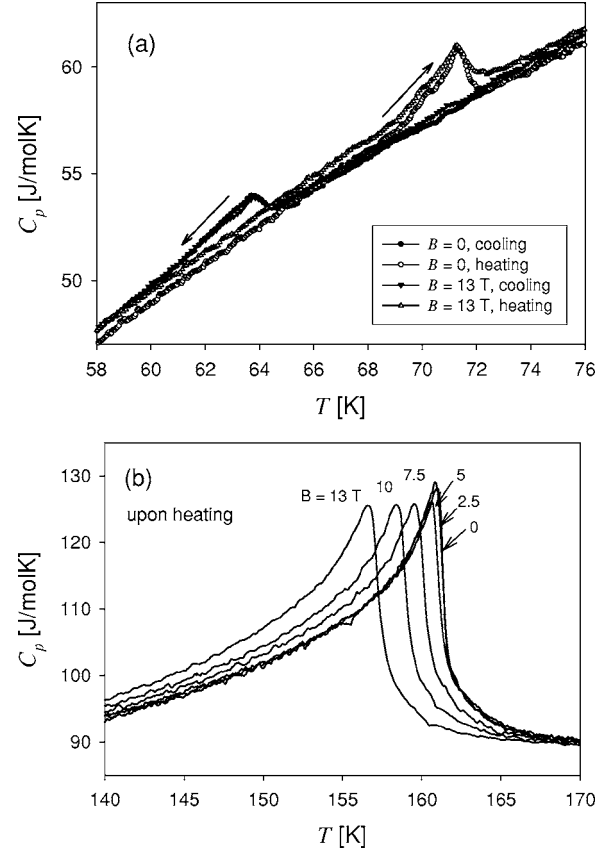


FIG. 4. The in-field specific heat of single-crystalline  $\text{UNi}_{0.5}\text{Sb}_2$  measured in the vicinity of the low-temperature anomaly (a) and near the AF phase transition (b). Magnetic field applied along the easy magnetization axis (i.e.,  $c$  axis).

character of the transition, and it is consistent with the presumption of its spin-reorientational nature. Furthermore, this behavior at  $T_{tr}$  has recently been confirmed by means of magnetic susceptibility and electrical resistivity measurements done on single-crystalline  $\text{UNi}_{0.5}\text{Sb}_2$ .<sup>3</sup> However, since the associated entropy jump constitutes only up to  $\sim 1.6\%$  of the  $R$  value, the spin reorientation is not expected to be profound.

The shape and position of the low-temperature anomaly were found to be independent of magnetic field at least up to  $B = 13$  T. The latter observation does not contradict the magnetic nature of this transition. The slope of the phase transition line  $B_{tr}(T)$  can be estimated from the magnetic version of the Clausius-Clapeyron relation

$$\frac{dB_{tr}}{dT} = \frac{\Delta S}{(-\Delta M)}, \quad (7)$$

where  $\Delta M$  is the jump in the magnetization curve. Taking its value from the data presented in Ref. 3 ( $\Delta M \approx 4.7 \times 10^{-8}$  J/T mol) we estimated the absolute value the  $B_{tr}(T)$  slope to be as high as  $2.8 \times 10^6$  T/K, which yields at  $B = 13$  T a shift in  $T_{tr}$  of  $\sim 5$   $\mu\text{K}$  only—i.e., far beyond our measurement accuracy.

On the contrary, upon applying a magnetic field the AF phase transition shifts considerably towards lower tempera-



tures, the faster the higher is the field value [see Fig. 4(b); there are shown the data from the first six runs only]. In a field of  $B=13$  T, the Néel temperature amounts to 156.8 K. At the same time, the shape and height of the anomaly are both nearly unaltered, even for the highest field applied. No measurable thermal hysteresis was found for any field strength. Such a behavior is characteristic of strongly anisotropic antiferromagnets with high values of the critical field for a metamagnetic transition. In this context, it is worthwhile to recall that indeed  $\text{UNi}_{0.5}\text{Sb}_2$  exhibits large anisotropy in its magnetic and electrical transport properties, in both the ordered and paramagnetic states, with the magnetization at 1.9 K being proportional to the magnetic field strength at least up to 5 T.<sup>3</sup> A more detailed description of the field dependence of the AF transition temperature will be given in Sec. III D.

### C. Isothermal magnetocaloric effect

Shown in Fig. 5 are the results of the magnetocaloric measurements taken on a single crystal of  $\text{UNi}_{0.5}\text{Sb}_2$  in the vicinity of the Néel temperature with magnetic field applied along the tetragonal  $c$  axis (the easy magnetization direction<sup>3</sup>). The measurements were done between the seventh and eighth temperature runs—i.e., at the time when the sample-Peltier cell connection was already mechanically stabilized due to thermocycling. The isothermal magnetocaloric coefficient  $M_T$  was found negative for all values of temperature and field strength. Thus, according to the formula

$$\Delta S(B) = - \int_0^B \frac{M_T}{T} dB, \quad (8)$$

the application of magnetic field results in an increase of the entropy [ $\Delta S(B) > 0$ ]; i.e., the magnetic system becomes less ordered. In the paramagnetic region the magnetocaloric coefficient is small and weakly dependent on both the field and temperature, even for temperatures only slightly above  $T_N(B=0) \equiv T_{N0} = 161.1$  K. In contrast, the  $M_T(B)$  curves taken in the very vicinity of  $T_{N0}$  on the low-temperature side show a substantial field and temperature dependence. At  $T = 160.7$  K (i.e.,  $\sim 0.4$  K below  $T_{N0}$ ) the magnetocaloric coefficient  $|M_T|$  first increases, goes through a broad maximum at  $B \approx 3$  T, and then slowly decreases in stronger magnetic fields. For the curves taken at  $T = 159.8$  K and 158.4 K the peak in  $M_T(B)$  is much more pronounced and shifted towards higher field values. Simultaneously, the slope of  $M_T(B)$  below the peak is decreasing with decreasing temperature. For the isotherms measured at  $T = 155.8$  K and below this temperature (see the bottom panel in Fig. 5) the peak is not visible. Moreover, the slope of these  $M_T(B)$  curves is gradually decreasing and becomes nonmeasurable for  $T = 100$  K. In particular, no magnetocaloric effect is observed around the low-temperature anomaly at  $T_r$  (not shown in the figure). Figure 5 shows the results taken upon increasing field only; upon decreasing the field some differences in the peak positions (up to 0.7 T) were noticed. This finding may be attributed solely to the finite value of  $K_{st}$  and the resulting temperature difference between the sample and thermal sink (we

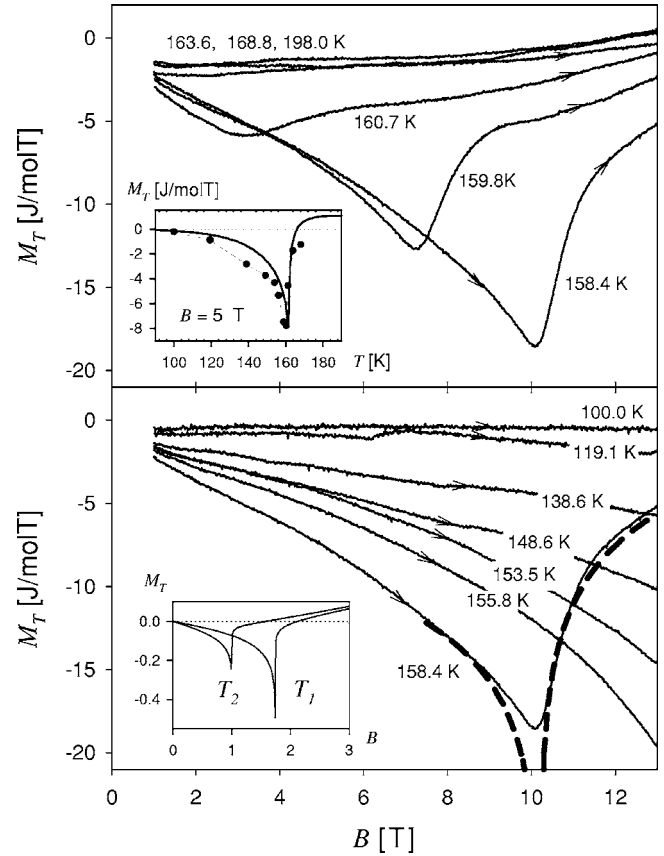


FIG. 5. Magnetic field dependence of the isothermal magnetocaloric coefficient for a  $\text{UNi}_{0.5}\text{Sb}_2$  single crystal measured with increasing magnetic field applied along the  $c$  axis. Top panel: data for  $T \geq 158.4$  K. Bottom panel: data for  $T \leq 158.4$  K. The inset in the top panel shows  $M_T$  measured at  $B=5$  T (points) and  $M_T$  calculated from the  $M(T)$  curve shown in Fig. 1 according to Eq. (11). The inset in the bottom panel shows the predictions for the  $M_T(B)$  dependence according to the 3D simple cubic AF Ising model;  $M_T$  and  $B$  are presented here in arbitrary units for two different temperatures with  $T_2 > T_1$  (see text for details). The dashed line in the bottom panel represents an exemplary logarithmic fit according to Eq. (12).

estimated this difference as being not larger than 0.15 K). The transition fields  $B_N$  given in the plot in the next paragraph were taken as an average of the data obtained for decreasing and increasing field.

In order to justify the experimental results for  $M_T(B)$  we made use of the 3D Ising model for the magnetic susceptibility  $\chi$ , taken from Ref. 10. The formula describing  $\chi(T)$  in the vicinity of the AF transition at zero field (see the dashed line in Fig. 1 close to  $T_N$ ) reads

$$\chi(T) \equiv M(T)/B \sim \frac{1}{T} [\xi_c - D_+(1 - T_{N0}/T) \ln |1 - T_{N0}/T|], \quad (9)$$

where  $\xi = 0.3397$ ,  $D_+ = 0.11$ , and  $D_- = 0.29$ . We assumed that at relatively low magnetic fields this formula will be modified only by the field dependence of  $T_N$ , for which we adopted its usual form for antiferromagnets:

$$\frac{T_{N0} - T_N}{T_{N0}} \sim B^2. \quad (10)$$

To make the next step we recall the thermodynamic relation between  $M_T$  and  $M$ :

$$M_T = -T \left( \frac{\partial M}{\partial T} \right)_B. \quad (11)$$

Using the above formula we tested the thermodynamical consistency of our results. The inset in the top panel of Fig. 5 confirms an agreement between measured  $M_T$  values and those calculated from  $M(T)$  curve taken at  $B=5$  T (see Fig. 1) according to Eq. (11).

Finally, we evaluated the expected shape of the anomaly in  $M_T(B)$  at the AF transition. The results are presented in the inset to the bottom panel of Fig. 5 for two different values of the temperature  $T_1 < T_2 < T_{N0}$ . The divergence at  $B_N$  is of logarithmic type, as for  $C_p(T)$ ; thus for  $|B - B_N| \ll 1$  we expect the following scaling law for AF materials:

$$M_T \sim M_T^0 + A_{MT}^\pm \ln|B - B_N|, \quad (12)$$

where  $M_T^0$  is an arbitrary constant and  $A_{MT}^\pm$  stand for the fluctuation amplitudes. At this place it is worthwhile to underline that the latter result does not depend on any particular choice of the model describing  $\chi(T)$ , and this is because all expressions for the susceptibility of antiferromagnets contain a singularity of the  $\tau \ln \tau$  type. Moreover, it also independent of the particular formula for  $T_N(B)$ , since the  $(T - T_N)$  variable could be always replaced by the  $(B - B_N)$  variable through a locally linear variable transformation (except for  $T = T_{N0}$ ).

An exemplary fit made using Eq. (12) is presented in the bottom panel in Fig. 5. The fitting was particularly successful on the high-field side of the transition—i.e., in the disordered phase. The qualitative agreement with the experiment is rather good (cf. the inset in the bottom panel of Fig. 5); however, the  $M_T(B)$  singularities at  $B_N$  in the experimental curves are somewhat smeared out, again due to limited values of  $K_{st}$ . This is the reason why we cannot present here a more detailed analysis of the magnetocaloric effect. Recently, we did manage to substantially improve our technology for sample thermal coupling (i.e., we obtained higher and more stable  $K_{st}$  values), and thus we intend to address the issue of the critical behavior of  $M_T(B)$  more thoroughly in our forthcoming studies.

#### D. Phase diagram and interaction anisotropy

Figure 6 summarizes all the data on the positions of the AF transition in  $\text{UNi}_{0.5}\text{Sb}_2$ , derived by means of specific-heat and magnetocaloric experiments. Apparently, agreement between the results of both methods is quite good. All the points form a square-root-like curve, as expected for antiferromagnets. However, the exact shape of this phase transition line depends much on details of the exchange interactions between the magnetic ions; in particular, it could be strongly affected by the magnetic anisotropy. The latter property is the primary point of interest for  $\text{UNi}_{0.5}\text{Sb}_2$ .

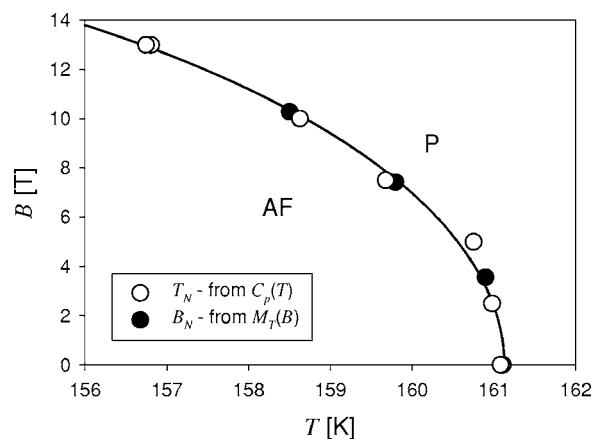


FIG. 6. The  $B$ - $T$  phase diagram of  $\text{UNi}_{0.5}\text{Sb}_2$  in the vicinity of the AF phase transition (for  $B$  applied along the easy magnetization axis). Open circles represent  $T_N$  data determined by means of specific-heat measurements. Solid circles correspond to  $B_N$  values derived from the isothermal magnetocaloric coefficient curves. The solid line is a fit according to Eq. (18).

To discuss the problem of magnetic anisotropy in  $\text{UNi}_{0.5}\text{Sb}_2$ , we have constructed a simple anisotropic, mean-field Ising-type model for spin  $S = \frac{1}{2}$ , which takes into account nearest-neighbor interactions only. Considering the tetragonal structure of the compound, it was assumed that the in-plane (four neighbors) and out-of-plane (two neighbors) interactions can be represented by positive  $J$  (ferromagnetic) and negative  $J_1$  (antiferromagnetic) exchange integrals, respectively. The schematic view of the modeled magnetic system is presented in Fig. 7, and the appropriate Hamiltonian is given by

$$H = -\frac{1}{2}J \sum_{\langle ij \rangle} S_i S_j - \frac{1}{2}J_1 \sum_{\langle ik \rangle} S_i S_k - B \sum_{i,k} (S_i + S_k), \quad (13)$$

where the first sum runs over nearest-neighbor pairs located in plane and the second term applies to pairs from adjacent planes. To find the phase transition line we reconstruct the Landau free energy associated with the above Hamiltonian. In the molecular field approximation it is easy to find the coefficients of the Landau expansions up to arbitrary order (see, for example, Ref. 14), but here we confine ourselves to present only four of them. The Landau free energy per site can be written in the form

$$f = f_0 + Gm_f + Wm_a^2 + W_1m_f^2 + Vm_fm_a^2, \quad (14)$$

where  $m_f = (m_1 + m_2)/2$ ,  $m_a = (m_1 - m_2)/2$ , and  $m_1$  and  $m_2$  are the magnetizations per site from odd and even planes, re-

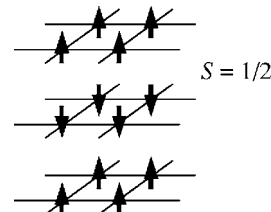


FIG. 7. Sketch of the modeled magnetic system.

spectively. The coefficients are given by the formulas

$$\begin{aligned}
 f_0 &= -T \left( \ln 2 + \frac{1}{2} a_0 \right), \\
 G &= -\frac{1}{2} T a_1, \\
 W &= 2J - J_1 - \frac{1}{2} T a_2, \\
 W_1 &= 2J + J_1 - \frac{1}{2} T a_3, \\
 V &= -\frac{1}{2} a_7
 \end{aligned} \tag{15}$$

and

$$\begin{aligned}
 a_0 &= 2 \ln \left[ \cosh \left( \frac{B}{T} \right) \right] \\
 a_1 &= \frac{4}{T} (2J + J_1) \tanh \left( \frac{B}{T} \right), \\
 a_{2,3} &= \frac{4}{T^2} (2J \mp J_1)^2 \left[ 1 - \tanh^2 \left( \frac{B}{T} \right) \right], \\
 a_7 &= \frac{16}{T^3} (-2J + J_1)^2 (2J + J_1) \tanh \left( \frac{B}{T} \right) \left[ \tanh^2 \left( \frac{B}{T} \right) - 1 \right].
 \end{aligned} \tag{16}$$

The phase transition was defined by the condition  $m_1 = m_2$ , which leads to the following equation for the  $B_N = f(T_N)$  line:

$$WW_1 - \frac{1}{2}VG = 0. \tag{17}$$

In the small-field limit this leads to the following set of expressions:

$$T_{N0} = 4J - 2J_1,$$

$$B_N^2 = \left( \frac{k_B}{\mu_B} \right)^2 T_N (T_{N0} - T_N) \left( \frac{T_N - T_{N0} - 4J_1}{8J} \right). \tag{18}$$

We underline that in Eqs. (15) and (16),  $T$  and  $B$  are expressed in terms of energy. We took into account that the energy associated with a spin  $S=1/2$  is equal to  $gS\mu_B B$  ( $g=2$  is the gyromagnetic factor,  $\mu_B$  the Bohr magneton). In order to explain the meaning of these formulas we indicate that for  $T \rightarrow T_{N0}$  the second of the above expressions could be simplified to the well-known square-root form

$$B_N^2 \approx B_{N0}^2 \left( \frac{T_{N0} - T_N}{T_{N0}} \right), \tag{19}$$

where

TABLE II. Parameters of the  $B_N = f(T_N)$  fit of the experimental data to Eq. (18). The  $B_{N0}$  value was calculated from Eq. (19).

$T_{N0}$	(161.1 ± 0.1) K
$J$	(35.8 ± 0.1) K
$J_1$	(-9.0 ± 0.2) K
$ J_1 /J$	0.25 ± 0.01
$B_{N0}$	(80 ± 3) T

$$B_{N0}^2 = T_{N0}^2 \left( \frac{k_B}{\mu_B} \right)^2 \frac{J_1}{2J}.$$

In a simple interpretation the  $B_{N0}$  parameter is the limiting field necessary to destroy the AF state at  $T=0$ . The results of the fitting of Eq. (18) to the data from Fig. 6 are presented in Table II. In this table we also included the  $B_{N0}$  value derived from the simplified formula represented by Eq. (19).

Applying the above model to  $\text{UNi}_{0.5}\text{Sb}_2$  we made several simplifying assumptions. First, the mean-field approach usually overestimates the transition temperature. Next, we used only one parameter to describe the out-of-plane interactions, despite the fact that the actual magnetic structure found in the  $^{121}\text{Sb}$  Mössbauer studies of  $\text{UNi}_{0.5}\text{Sb}_2$  is more complicated [the planes of ferromagnetically coupled uranium magnetic moments alternate in the sequence (+ - - +) along the  $c$  axis].<sup>2</sup> All these simplifications make the obtained numerical values of  $J$  and  $J_1$  less reliable; however, their ratio should reflect properly the anisotropy of the magnetic interactions. To support this statement it is worthwhile noting that the derived value for the  $|J_1|/J$  ratio is quite close to the value inferred from a rough estimation based on the square of the reciprocal interatomic U-U distances along the  $a$  and  $c$  axes, which amounts to 0.23 for both  $T=293$  K and 10 K.<sup>4</sup>

#### IV. SUMMARY

The specific-heat measurements on single-crystal  $\text{UNi}_{0.5}\text{Sb}_2$  have proved that the compound orders antiferromagnetically at  $T_N=161.1$  K and undergoes a subsequent spin-reorientation transition which appears to be highly hysteretic ( $T_{tr}=63.5$  K upon cooling and  $T_{tr}=71$  K upon heating), thus corroborating its first-order character. These results agree well with the magnetic and electrical transport data published in Ref. 3. The low-temperature transition was found to be independent of magnetic field. The entropy jump at  $T_{tr}$  is as small as  $\Delta S \sim 0.016R$ , which hints at a rather subtle change in the spin alignments.

The  $\lambda$ -shaped specific-heat anomaly at the AF phase transition was analyzed in terms of the critical fluctuations model with the critical parameter  $\alpha \approx 0^+$ . It was separated into a finite jump of the height  $\Delta C/R=1.8$  and a weak logarithmic divergence with the critical amplitude ratio  $A^+/A^- = 0.84$ . The value of  $\Delta C/R$ , together with the magnitude of the total magnetic entropy  $S_{magn} \approx R \ln 2$  released at  $T_N$ , suggests that the effective total angular momentum in the compound studied is equal to  $J=1/2$ . The derived value of  $A^+/A^-$  places  $\text{UNi}_{0.5}\text{Sb}_2$  somewhere between the 2D ( $A^+/A^- = 1$ ) and 3D ( $A^+/A^- = 0.52-0.54$ ) Ising systems.<sup>13</sup>

Application of magnetic field drives the AF transition towards lower temperatures, whereas the shape and height of the AF anomaly remain nearly unaltered. This field dependence of the specific heat leads to a strong magnetocaloric effect below  $T_N(B=0)$ . The isothermal magnetocaloric coefficient was found to be negative, thus implying a gradual destruction of the magnetic order by the external magnetic field. The  $M_T(B)$  curves measured just below  $T_N(B=0)$  cross over the AF-paramagnet phase transition line at some  $B_N(T)$  values. The shape of the anomaly observed at  $B_N$  is in qualitative agreement with a divergence of the  $M_T \sim \ln|B - B_N|$  type, predicted in the frame of the magnetic susceptibility formulas appropriate for different Ising models. At temperatures considerably lower than  $T_N(B=0)$  the anomaly in  $M_T(B)$  was shifted beyond the magnetic fields available in the experiments performed.

All the  $C_p$  and  $M_T$  results derived form together the AF-paramagnet phase transition line on the  $B$ - $T$  phase diagram. In order to analyze the anisotropic properties of  $\text{UNi}_{0.5}\text{Sb}_2$  we have constructed a simple mean-field model for the tetragonal lattice with FM coupling ( $J$ ) in the  $ab$  plane and AF coupling along the  $c$  axis ( $J_1$ ). Fitting the model formula to the  $T_N(B)$  and  $B_N(T)$  data yields the estimation for the exchange interactions anisotropy to be  $|J_1|/J=0.25$ .

#### ACKNOWLEDGMENTS

We are grateful to Professor J. Sznajd for the construction of the anisotropic mean-field model and fruitful discussions. This work was supported by the State Committee for Scientific Research (KBN) under research Grant Nos. 2 POB 036 24 (T.P.) and 4 T08A 04524 (D.K. and Z.B.).

- 
- <sup>1</sup>M. Brylak, M. H. Möller, and W. Jeitschko, *J. Solid State Chem.* **115**, 305 (1995).  
<sup>2</sup>D. Kaczorowski, R. Kruk, J. P. Sanchez, B. Malaman, and F. Wastin, *Phys. Rev. B* **58**, 9227 (1998).  
<sup>3</sup>Z. Bukowski, K. Gofryk, T. Plackowski, and D. Kaczorowski, *J. Alloys Compd.* **400**, 33 (2005).  
<sup>4</sup>Z. Bukowski, D. Kaczorowski, J. Stępień-Damm, D. Badurski, and R. Troć, *Intermetallics* **12**, 1381 (2004).  
<sup>5</sup>Z. Henkie and A. Misiuk, *Krist. Tech.* **14**, 539 (1978).  
<sup>6</sup>T. Plackowski, Y. Wang, and A. Junod, *Rev. Sci. Instrum.* **73**, 2755 (2002).  
<sup>7</sup>T. Plackowski, A. Junod, F. Bouquet, I. Sheikin, Y. Wang A. Jeżowski, and K. Mattenberger, *Phys. Rev. B* **67**, 184406 (2003).

- <sup>8</sup>T. Plackowski, *Phys. Rev. B* **72**, 012513 (2005).  
<sup>9</sup>M. F. Sykes and M. E. Fisher, *Physica (Amsterdam)* **28**, 919 (1962).  
<sup>10</sup>M. E. Fisher and M. F. Sykes, *Physica (Amsterdam)* **28**, 939 (1962).  
<sup>11</sup>C. Domb, *Adv. Phys.* **9**, 149 (1960).  
<sup>12</sup>J. J. Binney, N. J. Dowrick, A. J. Fisher, and M. E. J. Newman, *Theory of Critical Phenomena. An Introduction to the Renormalization Group* (Clarendon Press, Oxford, 1992).  
<sup>13</sup>V. Privman, P. C. Hohenberg, and A. Aharony, in *Phase Transitions and Critical Phenomena*, edited by C. Domb and J. L. Lebowitz (Academic Press, New York, 1991), Vol. XIV.  
<sup>14</sup>J. Sznajd, *J. Magn. Magn. Mater.* **42**, 269 (1984).